Generation of Spin Squeezing via Continuous Quantum Nondemolition Measurement

A. Kuzmich, L. Mandel, and N. P. Bigelow
Department of Physics and Astronomy, University of Rochester, Rochester, New York 14627
(Received 21 December 1999)

Continuous quantum nondemolition monitoring of a collective atomic spin with an off-resonant laser beam has been performed. Squeezed atomic spin states have thereby been produced with spin noise reduction to 70% below the standard quantum limit expected for a coherent spin state.

PACS numbers: 03.75.–b, 32.80.–t, 42.50.–p

During the last decade there have been rapid advances in atomic interferometry. One of the high points of these developments was the recent achievement of projection-noise-limited operation of a Cs atomic clock by Santarelli *et al.* [1]. In order to advance beyond the limit of accuracy imposed by the quantum projection noise in such a measurement one can use an *entangled* quantum state of the atoms. Recently the preparation of an entangled state of two ions has been reported [2] and a correlated state of two Rydberg atoms has also been prepared [3]. Parallel to these developments there has been interest in *multiatom squeezed spin states* (SSS) which are analogous to the squeezed states of light [4–6]. To this end, Hald *et al.* [7] recently reported preparation of an entangled multiatom state via quantum state transfer from squeezed light to a collection of atomic spins. We have also described [8] the creation of atomic samples with subshot-noise spin projection fluctuations, which were prepared using a quantum nondemolition (QND) measurement performed with optical probe pulses. In a related article, we have predicted [9] that such QND measurements, when performed on a spin-polarized sample of atoms, can produce a multiatom SSS.

In this Letter we report the experimental verification of these predictions. An important feature of the current work is in the use of *continuous* QND measurements to prepare the SSS. Consider the situation shown in Fig. 1. A beam of atoms of density ρ, spin polarized along the x axis, is moving with speed v through a light beam propagating along the z axis. For simplicity we assume that the atomic beam and the light beam have square profiles of the same size d along the y axis, while the atomic beam has width L along the z axis. Further, let us assume that the atomic spins are subjected to a time-dependent sinusoidal magnetic field $\mathbf{e}_y B\cos(\Omega t)$. The z component of $\hat{\mathbf{F}}(t)$ is given by $\hat{F}_z(t) = \cos[\phi(t)]\hat{F}_z^{(\mathrm{in})}(t) + \sin[\phi(t)]\hat{F}_x^{(\mathrm{in})}(t)$. Here $\hat{F}^{(\mathrm{in})}$ is the incident collective spin, $\phi(t) = \phi\sin(\Omega t)$, and we assume $\phi = (\mu B)/(\hbar\Omega) \ll 1$ so that $\hat{F}_z(t) \simeq \hat{F}_z^{(\mathrm{in})}(t) + \phi\sin(\Omega t)\hat{F}_x^{(\mathrm{in})}(t)$ (μ is the atomic magnetic moment).

For atoms with ground-state electronic angular momentum $\hbar/2$, the interaction Hamiltonian describing the measurement of the z spin projection $\hat{F}_z(t) = \sum \hat{F}_z^j$ (summation over individual spins) in an off-resonant atom-photon interaction scales [10] as $\sim\hat{s}_z(t)\hat{F}_z(t)$ and is of the QND type. Here $\hat{s}_z(t) \equiv \frac{1}{2}[\hat{a}_v^\dagger(t)\hat{a}_h(t) + \hat{a}_h^\dagger(t)\hat{a}_v(t)]$ and $\hat{a}_{h,v}(t), \hat{a}_{h,v}^\dagger(t)$ are annihilation and creation operators for vertically and horizontally polarized field modes. This QND-type interaction leads to polarization rotation of the probe light by an amount which is proportional to $\hat{F}_z(t)$. Let us introduce the observable $\hat{S}_y(\Omega) \equiv \int_0^T dt\, \hat{s}_y(t)\sin(\Omega t)$, which corresponds to the output of a spectrum analyzer that is being fed with the difference of photocurrents from the detectors D_1 and D_2, $\hat{s}_y(t) \equiv \frac{1}{2}[\hat{a}_v^\dagger(t)\hat{a}_v(t) - \hat{a}_h^\dagger(t)\hat{a}_h(t)]$. Here $T = 1/B$, where B is the resolution bandwidth of the spectrum analyzer. Measurement of $\hat{S}_y(\Omega)$ can be used to determine the spin rotation amplitude ϕ since $\langle\hat{S}_y(\Omega)\rangle = \phi\chi N\frac{P}{\hbar\omega}\tau$. Here $F^{(i)}$ is the total spin of one atom ($F^{(i)} = 4$ in our experiment), $\tau \equiv d/v$, $\chi = \frac{\sigma}{2A}g(D)\alpha_v$, σ is the atomic cross section for unpolarized light, $\alpha_v = 1/2$ is the dynamic vector polarizability of the Cs atom for our transition, and A is the cross section of the light beam, $g(D) \equiv \gamma D/(D^2 + \frac{1}{4}\gamma^2)$. D is the detuning of the field from the resonance and γ is the excited-state spontaneous decay rate. $N = \rho dvTL$ is the total number of atoms passing through the interaction region during time T and P is the optical power of the probe beam. The accuracy of the measurement can be written [11]

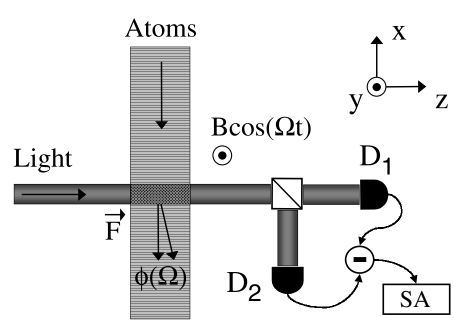

FIG. 1. Scheme for continuous QND measurement of a spin component.

 0031-9007/00/85(8)/1594(4)$15.00

$$\delta\phi = \frac{\sqrt{\langle(\Delta\hat{S}_y(\Omega))^2\rangle}}{|\frac{d}{d\phi}\langle\hat{S}_y(\Omega)\rangle|}. \tag{1}$$

In order to calculate the second moment of $\hat{S}_y$ we need the spin correlation function

$$\langle\hat{F}_z(t)\hat{F}_z(t')\rangle = \left(1 - \frac{|t - t'|}{\tau}\right)\rho V\langle(\Delta\hat{F}_z^{(i)})^2\rangle, |t - t'| \le \tau$$
$$= 0, |t - t'| > \tau, \tag{2}$$

where $\langle(\Delta\hat{F}_z^{(i)})^2\rangle$ is the variance of the z component of the spin for a single atom and $V = AL$ is the interaction volume. When the atom is spin polarized along the x axis, as we assume, $\langle(\Delta\hat{F}_z^{(i)})^2\rangle = F^{(i)}/2$. We then obtain

$$\langle(\Delta\hat{S}_y(\Omega))^2\rangle = \chi^2 F^{(i)} N\left(\frac{P}{2\hbar\omega}\right)^2 \frac{\sin^2(\frac{1}{2}\Omega\tau)}{\Omega^2} + \frac{P}{8\hbar\omega B}, \tag{3}$$

where the first and second terms are due to (atomic) spin noise and photon shot noise, respectively. The measurement accuracy of the spin rotation angle can be written

$$\delta\phi = \frac{2}{\sqrt{F^{(i)}N}}\sqrt{\frac{\sin^2(\frac{1}{2}\Omega\tau)}{(\Omega\tau)^2} + \frac{\hbar\omega}{2(\chi\tau)^2 N F^{(i)} P B}}. \tag{4}$$

When $\frac{\hbar\omega}{2(\chi\tau)^2 N F^{(i)} P B} \ll 1$, the photon shot noise corresponding to the last term under the square root sign is much smaller than the atomic noise and can be neglected. The spin noise (normalized to its value at $\Omega = 0$) plotted as a function of $\Omega\tau$ is shown in Fig. 2. In this case, for low frequencies ($\Omega \ll 1/\tau$), we find that the measurement accuracy is given by the standard quantum limit (SQL), $\delta\phi_{\mathrm{SQL}} = 1/\sqrt{F^{(i)}N}$. As the frequency Ω of the applied spin rotation increases, the phase uncertainty $\delta\phi$ falls below the SQL and the accuracy limit on the achievable uncertainty is set by the photon shot noise of the probe. However, if the collective atom-photon coupling is high enough [12], the limit is determined by the backaction of the probe photons onto the collective atomic spin. The measurement accuracy of the spin rotation angle is then at the Heisenberg limit $1/N$ [9]. The high frequency behavior of the noise is key to our realization of spin squeezing and to our measurement of spin noise which is below the SQL.

Under the conditions of our experiment, we do not have a beam of atoms of definite velocity v traveling in a given direction. Rather, we have a Maxwell-Boltzmann distribution of velocities of atoms crossing the QND probe beam. We can include this velocity spread by averaging $\langle\hat{S}_y(\Omega)\rangle$ and $\langle(\Delta\hat{S}_y(\Omega))^2\rangle$ over the velocity distribution $p(\mathbf{v}) = m^{3/2}/(2\pi T^{3/2})\exp[-m(v_x^2 + v_y^2 + v_z^2)/2T]$. Here m is the atomic mass and T is the temperature. We approximate the probe beam by a cylinder of radius R and length $L \gg R$ having uniform transverse intensity distribution, and we make an additional approximation in taking each atom to travel the distance $\sqrt{2}R$ through the beam in a transverse plane. The spin noise given by Eq. (3) for Cs atoms at temperature $T = 295$ K averaged over all velocities with $R = 50\ \mu$m is plotted in Fig. 3. Just as for the monochromatic atomic beam (Fig. 2), the measured spin noise drops to zero at high frequencies, while it is at the shot-noise level at $\Omega = 0$.

An outline of our experimental setup is shown in Fig. 4. A paraffin-coated glass cell contains the Cs atoms. Under the conditions of our experiment, the measured lifetime of spin polarization in the cell is on the order of 1 s. It is important initially to prepare the atomic sample in a coherent spin state (CSS). Two important features of the CSS are that (i) it is fully spin polarized along some direction (and therefore has maximum coherence) and (ii) spin fluctuations of the sample are at the shot-noise level given by $\sqrt{F/2}$, where F is the value of the collective spin.

The major part of the light from an extended cavity diode laser DL3 is used as our QND probe. The QND-probe beam is detuned about 900 MHz from the center of the $6S_{1/2}, F = 4 \rightarrow 6P_{3/2}$ transition(s). This 1 mW light beam is focused into the gas cell with Gaussian waist of 100 μm. Note that the optical pumping beams and the probe beam do not spatially overlap. The probe beam is then refocused by lens L2 onto a Glan-Thompson polarizing beam splitter (PBS) whose outputs are measured by two (85% quantum efficiency) photodiodes D_1 and D_2.

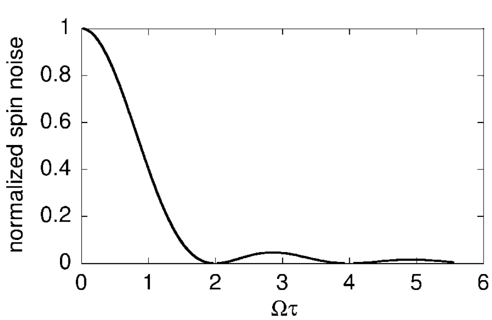

FIG. 2. Theoretical spectrum of the spin noise for a monochromatic atomic beam.

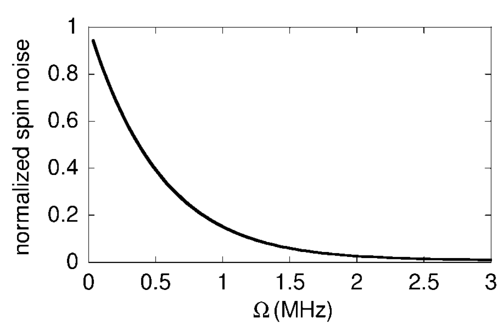

FIG. 3. Calculated spectrum of spin noise for Doppler broadened Cs vapor at $T = 295$ K, with a 100 μm diam QND-probe laser beam.

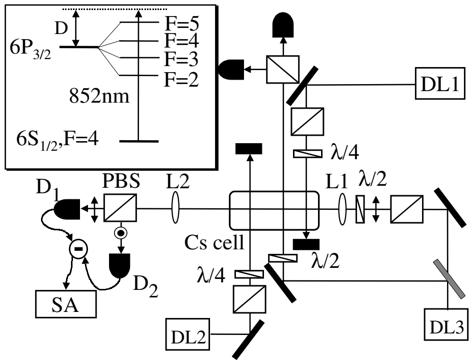

FIG. 4. Outline of the experimental setup. Not shown are 3 pairs of coils to produce dc magnetic fields and a coil producing rf magnetic field. The inset shows the level diagram for the QND probe beam. See text for details.

The outputs of the photodiodes are amplified, and the difference signal is fed into a spectrum analyzer SA, where noise spectra between 3 and 20 MHz are recorded. By comparison with the noise produced by a thermal light source of equal dc photocurrent, we find that for all three lasers the amplitude noise is at the shot noise level to within 5% for 1 mW of optical power. By analyzing an unfocused light beam transmitted through the atomic cell with the atoms spin polarized along the beam we found that the QND-probe laser did not contribute excess phase noise for given power (1 mW) and detuning (900 MHz) off the Doppler absorption profile. The lasers only contributed significant amount of excess amplitude and phase noise at lower (<3 MHz) frequencies.

We note that our use of lasers with shot-noise amplitude fluctuations for optical pumping should result in shot-noise level samples of atomic spins. Moreover, since the lifetime of the spin polarization in the cell is long (~1 s) compared with the periods of interest (<0.3 μs), the pump fluctuations are suppressed even more—by several orders of magnitude in power for spin fluctuations relative to photon fluctuations. In our experiment two 852 nm diode lasers DL1 and DL2 are used to spin polarize the atomic medium. Both light beams are circularly polarized with the same helicity and propagate along the direction of the magnetic field of several Gauss. The laser DL1 of about 3 mW average power (adjusted with a neutral density filter) is tuned to the $6S_{1/2}, F = 3 \rightarrow 6P_{3/2}$ transition(s), while the laser DL2 of less than 100 μW average power is tuned to the $6S_{1/2}, F = 4 \rightarrow 6P_{3/2}$ transition(s). A small portion of the linearly polarized light from laser DL3 is split off and used to monitor the degree of spin polarization. This probe beam propagates through the cell along the direction of spin polarization. By scanning the frequency across the Doppler profile, we measure the dispersive profile of the polarization rotation angle and the Lorentzian profile of the absorption. We aligned the magnetic field (and therefore also the spin polarization) orthogonally to the QND-probe beam with the help of the Faraday rotation signal in the dc channels of our homodyne detectors on the QND probe. The degree of spin polarization of the atoms was >95%.

An important aspect of our spin squeezing experiment is the need to identify the spin shot-noise level. By analogy with the use of thermal light for the photon shot-noise normalization [13], we make use of the unpolarized atoms as a benchmark for the spin shot noise. In a previous experiment, we have shown [8] that the spin noise of unpolarized atoms in a cell scales linearly with the number of atoms, as expected for an uncorrelated sample. Because our Cs atoms have total spin $F = 4$ instead of elementary $1/2$ spins, the spin noise of an unpolarized collection of atoms is $\frac{2}{3}(F + 1)$ times larger than the spin noise of the CSS with an equal number of atoms.

As described above, the spin shot noise can be directly measured at $\Omega = 0$. From the experimental point of view, however, the measurement of noise at $\Omega = 0$ is complicated by the fact that our probe laser has a large amount of excess amplitude and phase noise at frequencies below 3 MHz. To avoid this problem, we apply a uniform magnetic field in a direction perpendicular to the QND-probe propagation. In this case, one can show that the correlation function (2) becomes

$$\langle \hat{F}_z(t)\hat{F}_z(t')\rangle|_{B\neq 0} = \frac{1}{2}\cos\omega_L(t - t')\langle \hat{F}_z(t)\hat{F}_z(t')\rangle|_{B=0}\,. \tag{5}$$

Here $\langle \hat{F}_z(t)\hat{F}_z(t')\rangle|_{B=0}$ is given by Eq. (2). The effect of the applied magnetic field is that the spin noise now manifests itself at the Larmor precession frequency ω_L and the net amount of observed noise is reduced by one-half. The spectrum of the total noise, normalized to the photon shot noise of the probe, is shown in Fig. 5, curve (a). Here $B = 15$ G, so that $\omega_L \simeq 5$ MHz.

From this measurement, made with unpolarized atoms, we can obtain the shot-noise level for the CSS: First we remove photon shot-noise contribution from the QND probe. Next, we take into account the factor of $\frac{2}{3}(F + 1)$ for the difference between the expected shot noises of an unpolarized sample of atoms and for the CSS, a factor of $\frac{1}{2}$ in Eq. (5), and we also account for the fact that after optical pumping we have $16/9$ times more atoms in the $F = 4$ state than in the unpumped cell (this population distribution was confirmed experimentally in absorption measurements). The resulting SQL spin noise level for the CSS is shown in Fig. 6 by the dashed line. The magnitude of the spin noise peak (and so, the accuracy of determination of the SQL spin noise level) varied less than 5% from run to run.

Next, we repeat the measurement on the sample after spin polarizing the atoms by optical pumping. For spin polarized atoms, the correlation function of Eq. (5) is modified and becomes for $|t - t'| \leq \tau$

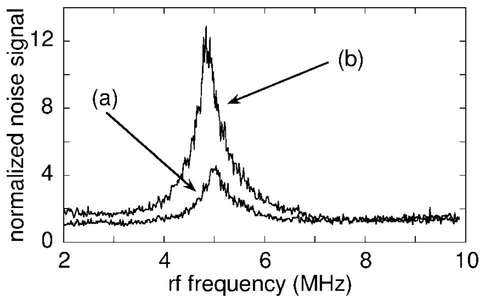

FIG. 5. Measured noise spectrum. (a) Atoms are unpolarized. (b) Atoms are spin polarized.

$$\langle \hat{F}_z(t)F_z(t')\rangle_L = \frac{1}{2}\cos\omega_L(t-t')\left(1-\frac{|t-t'|}{\tau}\right) \times \left\{\rho V\langle(\Delta F_z^{(i)})^2\rangle + \chi^2\langle\hat{F}_x\rangle^2\frac{P\tau}{4\hbar\omega}\left[1-\left(\frac{\sin(\omega_L\tau)}{\omega_L\tau}\right)^2\right]\right\}. \tag{6}$$

Measuring the noise spectrum for the CSS [Fig. 5(b) with magnetic field being slightly lower than in Fig. 5(a)], we observe a much larger noise peak due to the "backaction" of the probe [the extra term on the right in Eq. (6)]. The absolute magnitude of the resulting noise agrees (to better than a factor of 2) with theoretical estimates derived from Eqs. (3), (5), and (6); however, more quantitative comparison is made difficult by the approximations we made in deriving Eq. (3).

Having determined the SQL for the spin noise of the sample and having understood the noise for the polarized vapor, we next directly demonstrate the low-noise character of the collective atomic spin as prepared by the continuous QND measurement. To do this we first reduce the magnetic field back to 2 G and then we apply an rf magnetic field along the y axis whose frequency is >3 MHz and $>\omega_L$. The rf field produces a small oscillation of the collective atomic spin along the z axis which we then detect. In Fig. 6, we show the spin noise spectrum observed under these conditions. As mentioned above, the dashed line defines the SQL of the spin projection measurement for the CSS. In this example, we applied the rf modulation at 16 MHz. The peak in the spectrum is the measured spin rotation due to the applied rf field. Clearly, the resulting spin interferometer is delivering the subshot-noise performance with a $\sim$70% noise reduction below the SQL. Similar results were obtained for other rf modulation frequencies.

In conclusion, we have proposed and implemented a continuous QND measurement of spin projection as a way of preparing squeezed spin states of atoms. We have obtained about 70% of spin noise reduction in a sample of about 10^7 atoms and measured a small spin rotation with

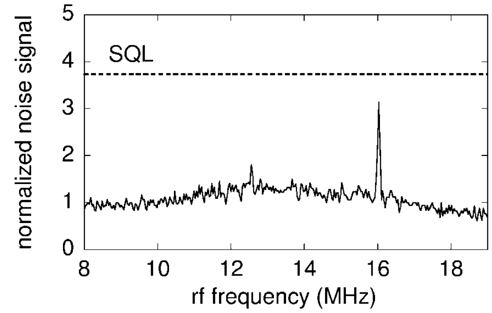

FIG. 6. Measured spin noise spectrum. The dashed line indicates the SQL accuracy of spin rotation measurement. The peak at 16 MHz is due to spin rotation by the applied rf field and is a demonstration of subshot-noise atomic interferometry.

an accuracy exceeding the SQL of the phase (angle) measurement. An important difference between our technique and others lies in the fact that the same laser beam serves simultaneously for the preparation of the SSS and for measurement of the spin rotation signal. The simplicity of our technique should help the application of the SSS to other situations, such as cold trapped atoms and Bose-Einstein condensates. In each of these cases, as in our vapor-cell experiment, the conditions for an optically thick sample of atoms can be readily satisfied, which should result in significant amounts of spin squeezing.

We acknowledge useful discussions with I. A. Walmsley, E. S. Polzik, E. B. Alexandrov, and W. Happer. We also thank E. B. Alexandrov for providing the paraffin-coated Cs cell used in this experiment. This work was supported by the National Science Foundation, the U.S. Office of Naval Research and the David and Lucile Packard Foundation.

[1] C. Santarelli *et al.,* Phys. Rev. Lett. **82**, 4619 (1999).
[2] Q. A. Turchette *et al.,* Phys. Rev. Lett. **81**, 3631 (1998).
[3] E. Hagley *et al.,* Phys. Rev. Lett. **79**, 1 (1997).
[4] M. Kitagawa and M. Ueda, Phys. Rev. Lett. **67**, 1852 (1991); Phys. Rev. A **47**, 5138 (1993).
[5] D. J. Wineland *et al.,* Phys. Rev. A **46**, R6797 (1992); **50**, 67 (1994).
[6] G. S. Agarwal and R. R. Puri, Phys. Rev. A **41**, 3782 (1990); A. Kuzmich *et al.,* Phys. Rev. Lett. **79**, 4782 (1997); E. S. Polzik, Phys. Rev. A **59**, 4202 (1999); K. Mølmer, Eur. Phys. J. D **5**, 301 (1999).
[7] J. Hald *et al.,* Phys. Rev. Lett. **83**, 1319 (1999).
[8] A. Kuzmich *et al.,* Phys. Rev. A **60**, 2346 (1999).
[9] A. Kuzmich *et al.,* Europhys. Lett. A **42**, 481 (1998).
[10] W. Happer and B. S. Mathur, Phys. Rev. Lett. **18**, 577 (1967).
[11] B. Yurke, Phys. Rev. Lett. **56**, 1515 (1986).
[12] Strong collective atom-photon coupling can be achieved through the use of either optically thick atomic samples or optical cavities.
[13] Ling-An Wu *et al.,* Phys. Rev. Lett. **57**, 2520 (1986).